JOURNAL OF THE ROYAL SOCIETY Interface

A hybrid polymer gel with controlled rates of cross-link rupture and self-repair

Farrell R Kersey, David M Loveless and Stephen L Craig

J. R. Soc. Interface 2007 **4**, 373-380
doi: 10.1098/rsif.2006.0187

JOURNAL OF THE ROYAL SOCIETY Interface

J. R. Soc. Interface (2007) **4**, 373–380
doi:10.1098/rsif.2006.0187
Published online 8 December 2006

A hybrid polymer gel with controlled rates of cross-link rupture and self-repair

Farrell R. Kersey, David M. Loveless and Stephen L. Craig*

Department of Chemistry and Center for Biologically Inspired Materials and Material Systems, Duke University, Durham, NC 27708-0346, USA

A family of hybrid polymer gels is described, in which covalent cross-links create a permanent, stiff scaffold onto which reversible metal–ligand coordinative cross-links are added. The reversible metal–ligand interactions are shown to bear mechanical stress within the hybrid gel, and relaxations in response to that applied stress are consistent with the stress-free kinetics of ligand exchange in systems that model the reversible cross-links. The stress-induced dissociation of a model metal–ligand complex is examined by a single-molecule force spectroscopy, and its mechanical response is compared with a previously studied complex. The mechanical response of the individual interactions is relevant to those found in the family of hybrid gels, and the modular platform is therefore suitable for the study of stress-induced molecular dissociations, and their subsequent repair, within a macroscopic material of fixed structure.

Keywords: polymer gels; self-repair; force spectroscopy

1. INTRODUCTION

The majority of strategies towards the repair of materials and the recovery of mechanical properties fall broadly into one of two general categories. First, self-healing can be effected by the *creation* of new chemical bonds within the material, an example of which involves the release and *in situ* polymerization of monomers in a crack, as demonstrated in elegant work by White *et al.* (2001). Second, damage can be repaired by the *re-creation* of what are essentially the same chemical bonds that are ruptured in the damage event. Chen *et al.*'s (2002) recent demonstration of thermally re-mendable polymers based on cycloaddition (Diels–Alder) reactions falls into this category.

In the latter strategy, the loss of stress-bearing entanglements must occur through bond rupture that is reversible, and the bonds must break in a way that does not lead to subsequent, mechanically unproductive reactions prior to being reformed. Free radicals, such as those produced in homolytic bond scission reactions, are clearly undesirable in this regard. The Diels–Alder-based polymers represent a clever solution to this challenge, because they presumably circumvent free-radical formation through concerted bond rupture mechanisms, i.e. retro-Diels–Alder. In addition to avoiding unwanted side reactions, the re-creation chemistry must not only be thermodynamically favourable, but must also be kinetically accessible on the time-scale of crack propagation. The necessary kinetics might be achieved with an external stimulus, for example heat (as in the Diels–Alder polymers) or light, but autonomic systems (those that function without an applied external stimulus) are clearly desirable.

The use of rapidly reversible, non-covalent interactions (Zimmerman *et al.* 1998; Moore 1999) such as hydrogen bonds or metal–ligand coordination has been suggested to be a possible mechanism for endowing materials with self-healing character that does not require an external stimulus. This latter equilibrium polymer strategy is conceptually charming, but it is compromised in practice by the simultaneous requirements of reversibility and memory of an initial structural state; water is self-repairing, but fairly useless as a structural material. To preserve a desired structure, reversible interactions might be combined in a composite material with components that preserve a memory of the desired state: encasement within an exoskeleton; tethering to an endoskeleton; or with an additional 'fixed' system in an interpenetrating network.

Nature, not surprisingly, appears to use strategies of both creation and re-creation in her own solutions to the self-healing problem. Most common are the active mechanisms of creating a new material; for example, tissue damage often triggers metabolic pathways that remodel and regenerate the damaged, nascent biomaterial. But nature also appears to use the re-creation approach to her advantage, through the sacrifice and subsequent regeneration of non-covalent bonds in a manner similar to that described previously. Thompson *et al.* (2001) have used a force microscope tip to look at energy dissipation during bone indentation. They found that, below a threshold force value, the indentation

*Author for correspondence (stephen.craig@duke.edu).

One contribution of 9 to a themed supplement 'Self-healing polymers and composites'.

Received 8 October 2006
Accepted 4 November 2006

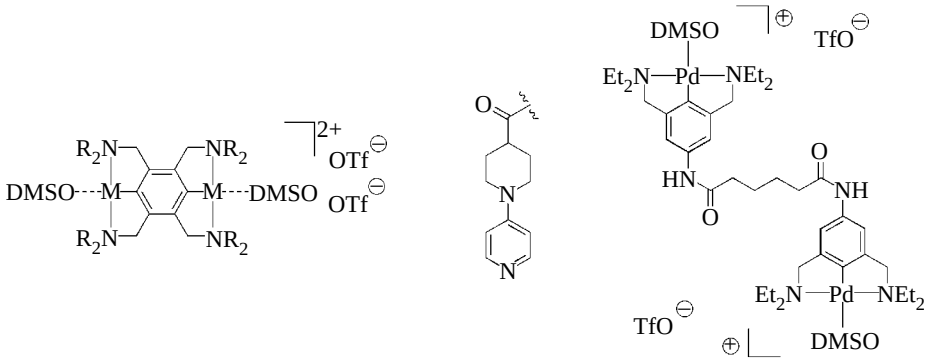

1a M = Pd R = Me
1b M = Pd R = Et
1c M = Pt R = Me
1d M = Pt R = Et

2 **3**

Scheme 1. Structure of cross-linkers **1** employed in this work. Ligand moiety **2** was attached via an amide linkage to tethered PEG chains in single-molecule force spectroscopy experiments. Cross-linker **3** bears the same functional groups as **1b** and was used in a related previous work (Yount *et al.* 2005; Kersey *et al.* 2006).

energy was dissipated on a time-scale of approximately 30 s and that the initial bone toughness was recovered after the indentation force was removed. The kinetics of sacrifice and repair are similar to relaxation kinetics found in the collagen matrix within which hydroxyapatite crystals are deposited, implying that inter-strand collagen 'bonds' are sacrificed in response to a compressive force and then subsequently repaired once the force is removed. The cellular scaffold and the presence of the minerals within the composite bone presumably provide the permanent framework that facilitates a load-bearing function.

Nature's successful design strategy inspires the 'forward engineering' of alternative, synthetic materials. The construction of such materials is necessarily multi-faceted. First, the critical reversible interactions must be presented within an irreversible macroscopic structure. Second, the reversible interactions within the hybrid material must bear stress in a way that contributes to the mechanical properties. Under a sufficiently high load, the reversible interactions must yield prior to the failure of the 'permanent' component. Furthermore, they must yield in a manner that relieves stress on the permanent framework, and they must be able to reform once the applied stress is removed. In this respect, understanding and controlling both the failure (in the presence of an applied external force) and the repair (in the absence of an applied external force) rates of the reversible interactions within the hybrid material are essential. Well-characterized molecular and material platforms, in which systematic structural variations are possible, might facilitate the development of hybrid self-healing materials.

Here, we describe a hybrid polymeric scaffold in which many of the aforementioned criteria are met. The permanent, structural component is a polymer network created by covalent cross-links between polymer chains. The reversible, potentially self-healing component is a metal–ligand coordination complex between a bifunctional Pd(II) or Pt(II) pincer complex, **1**, and a polymer side-chain pyridine ligand, **2** (scheme 1). We note that Pollino *et al.* (2004) also have used pincer complexes as polymeric cross-linkers in combination with other side-chain functionalization strategies (Pollino & Weck 2005). In the present work, the *N*,*C*,*N*-pincer complexes have the mechanistic advantage that their dynamic response, which is related to the kinetics of ligand exchange, can be varied independently of the thermodynamics of complexation. For example, we have previously reported that the association constants for the recognition units in **1a**·**2** and **1b**·**2** in dimethylsulphoxide (DMSO) are 1600 and 1300 M^{-1}, respectively, but the solvent-assisted ligand dissociation rate of the former is nearly two orders of magnitude greater than that of the latter (70–100 versus 1.0 s^{-1}; Yount *et al.* 2005). Similar effects are observed with the Pt(II) complexes **1c** and **1d**. The variance in pyridine off-rates creates a phenomenological 'kinetic isotope effect' through which the contributions of bond rupture to polymer mechanical properties can be evaluated directly. In many cases, those bond rupture events are adequately described without considering the effect of a mechanical stress on the rupture event (Yount *et al.* 2005).

The apparently minimal contributions of mechanical stress on bond rupture rates need not be general, and in fact (given the importance of bond scission events in polymer failure) there are clearly situations in which the applied force will have a dramatic and critical effect on the rate of bond breaking in the material. The pincer–pyridine complexes are also advantageous in this regard, in that the dynamic mechanical response of the coordinative bond can be observed by a single-molecule force spectroscopy (SMFS). We have recently reported that dissociation under dynamic load of the reversible bond between a Pd(II) pincer complex **3** (scheme 1) and two different pyridine ligands is well correlated with the thermal exchange rates measured independently for metal–ligand complexes that model those used in the SMFS experiments (Kersey *et al.* 2006). The rupture forces observed by SMFS are apparently kinetically determined, and we examine here the SMFS of the Pd(II)–pyridine complex **1a**·**2**, which differs from the **3**·**2** complex studied previously,

in that dimethylamino, rather than diethylamino, substituents are adjacent to the metal centre at the ligand-binding site. The decreased sterics in **1a·2** are significant, in that they increase the rate of the associative ligand-displacement mechanism by nearly two orders of magnitude, but have only a modest effect on the association constant of the complex in DMSO (Yount *et al.* 2005). Thus, kinetic contributions to properties—both in single molecules and within bulk material—can be clearly distinguished from thermodynamic contributions. The two complexes also differ, in that **1a·2** possesses an unsaturated spacer, which could possibly lead to cooperative binding due to closely coupled metal centres. Previous work carried out in our group, however, suggests that the metal sites are independent of one another in both thermodynamics and kinetics, and that the differences in the spacers do not influence the coordination interaction (Jeon *et al.* in press). The complex of **1a** with **2** was chosen as the model pincer–pyridine complex in SMFS experiments, because the lifetimes of complexes with less nucleophilic pyridines are too short on the timescale of the SMFS experiments. Previous work, however, suggests that the SMFS of **1a·(2)$_2$** can be scaled reliably to that of complexes containing less nucleophilic pyridine ligands (Kersey *et al.* 2006), and hence comparisons of **1a·2** are likely to be directly relevant to the cross-linking interactions of **1a** with pyridine side chains in the 4-vinylpyridine-based polymer gels and networks described in §§ 2.5 and 3.

With the characterization of both the relative mechanical properties (strain-induced rupture) and the ligand-binding kinetics (bond re-creation) of two homologous pincer–pyridine complexes in hand, these complexes (and their related Pt(II) analogues) are introduced as potential, additional cross-linking interactions into covalently cross-linked, stiff polymer gels. Dynamic mechanical analysis of the gels reveals that the metal–ligand coordination bonds function as reversible, stress-bearing entanglements in the network. Initial features of a self-healing hybrid polymer are met, and the system is well-suited to further systematic structure–activity relationships.

2. EXPERIMENTAL

2.1. Materials

3-Aminopropyltriethoxysilane (APTES), hexanoic anhydride, PYBOP, DMSO, pyridine, 4-(dimethylamino)pyridine (DMAP) and triethylamine were purchased from Acros and used as received. Piperidine (peptide synthesis grade) was purchased from Perkin Elmer and used as received. CH_2Cl_2 and *N*,*N*-dimethyl formamide (DMF) were purchased from Fisher Scientific and were made anhydrous by running through solvent drying columns prior to use. Toluene and $CHCl_3$ were purchased from Fisher Scientific, stirred with $MgSO_4$ and filtered through a pad of $MgSO_4$ to remove residual water prior to use. Absolute ethanol was purchased from Aaper Alcohol and Chemical Co., and deionized water was obtained from a Millipore filtering system.

2.2. Cantilever and surface funtionalization

All sample preparations were performed in glass scintillation vials. Si_3N_4 cantilevers (Thermomicroscopes, Sunnyvale, CA, model AUHW) and polished SiO_2 substrates (1.5×1.5 cm) were cleaned with piranha solution (7 : 3 H_2SO_4 : H_2O_2 (30%) by volume) for 30–45 min, rinsed with water and ethanol, dried under a stream of N_2 and oven-dried for 5 min at 120°C to remove residual solvent (after each rinsing, cantilevers were dried by touching them against a kimwipe). *Caution should be used when handling piranha solution; it has been reported to detonate unexpectedly.* Cantilevers/substrates were subsequently incubated in 1–3% APTES in either dry CH_2Cl_2 or dry toluene for 2 h, followed by rinsing with the same solvent. Substrates were then sonicated for 5 min in the same solvent to remove residual APTES, rinsed with the solvent and dried under a stream of N_2.

Cantilevers and substrates were then incubated in 1 mM NHS-PEG-Fmoc (Nektar Therapeutics, Huntsville, AL, M_w=3501 Da, PDI=1.01) in dry $CHCl_3$ for 30–60 min. Following PEG attachment, cantilevers/substrates were rinsed with $CHCl_3$ and ethanol, and dried under a stream of N_2. Following this step, the terminal Fmoc group was removed by incubating cantilevers/substrates in 20% piperidine in dry DMF for 20–30 min, and samples were subsequently rinsed with DMF and ethanol, dried under a stream of N_2 and oven-dried for 5 min at 120°C to remove residual solvent. For attachment of **2**, cantilevers/substrates were placed in a 3 ml dry DMF solution containing **2**, PYBOP, pyridine, and 0.5 ml triethylamine that was heated at approximately 85°C for 4 min until **2** went into solution, and samples were subsequently incubated overnight at room temperature, yielding **2**-functionalized samples. After reactions with **2**, cantilevers/substrates were rinsed with DMF and ethanol, dried under a stream of N_2 and oven-dried for 5 min at 120°C to remove residual solvent. Finally, cantilevers/substrates were incubated in 10 mM solutions of hexanoic anhydride in dry CH_2Cl_2 with 0.5 ml triethylamine for 1 h. Cantilevers/substrates were then rinsed with CH_2Cl_2 and ethanol, and substrates were sonicated for 5 min in ethanol to remove physisorbed molecules, rinsed with ethanol and dried under a stream of N_2. Following the preparation, cantilevers and substrates were either used immediately or stored below 0°C.

2.3. Single-molecule force spectroscopy

Force spectroscopy was carried out using an MFP-3D atomic force microscope (Asylum Research, Santa Barbara, CA) in contact mode at room temperature. Triangular cantilevers with spring constants (k_c) ranging between 30 and 102 pN nm^{-1} were used. The spring constant of each cantilever in DMSO was determined using the thermal noise method as previously described (Hutter & Bechhoefer 1993). To correct for viscous drag, forces were determined by taking the difference between the force at rupture and

the average force between the approach and the retract curves (Janovjak *et al.* 2005).

Approximately 30 ml of a DMSO solution of **1a** were pipetted onto the substrate prior to performing experiments. Measurements were performed in an open atmosphere with scanning set for approach/retract cycles. A sensor in the AFM scanner monitored the sample temperature, which varied no more than ± 1°C during each experiment. Each experiment was repeated with different samples on different days. Force curves were collected and analysed using Igor Pro (v. 5.0, Wavemetrics). For each loading rate, approximately 250–600 force curves were collected at different locations on the surface. All force curves were converted from deflection–tip displacement plots into force–separation curves using the MFP-3D software provided by Asylum Research. Loading rates were calculated from the product of the piezo retract velocity with the cantilever spring constant ($r_f = k_c v_r$).

The logarithmic plots of most probable force (F^*) versus $\ln(r_f)$ were fitted with the Bell–Evans model (equation (2.1)), where $k_B T$ is the thermal energy (4.11 pN nm); x_β is the effective distance between the bound state and the transition state, projected along the vector of applied force; r_f is the force-dependent loading rate; and k_d is the thermal off-rate at zero force (Bell 1978; Evans 1997, 2001),

$$F^* = \frac{k_B T}{x_\beta} \ln(r_f) + \frac{k_B T}{x_\beta} \ln\left(\frac{x_\beta}{k_d k_B T}\right). \qquad (2.1)$$

2.4. Statistical analysis

All kernel density function (KDF) plots of rupture forces were created using the freeware statistical package R (http://www.r-project.org/; plugin.density package) as previously described (Vander Wal *et al.* 2006). Density curves were generated using 512 points. The KDF plots were fitted with Gaussian distributions using Igor Pro (v. 5.0), and the peak of the Gaussian distribution was used for F^*.

2.5. Polymer gel synthesis and dynamic mechanical analysis

In a 1 mm thick glass polymerization chamber were mixed 0.500 ml 4-vinylpyridine (4-VP), 0.500 ml hydroxyethylmethacrylate (HEMA), 0.002 ml ethylene glycol dimethacrylate (EGDMA), 0.300 ml ethylene glycol, 0.200 ml H_2O, 0.100 ml of 400 mg ml^{-1} aqueous ammonium persulphate and 0.100 ml of 150 mg ml^{-1} aqueous sodium metabisulphite. The ensuing polymerization was allowed to continue for 20 h, after which time the slab of polymer was removed and placed in DMSO for 5 days. The solvent was changed each day to remove low-molecular weight components. The hydrogel was then cut with biopsy punches (6 mm in diameter) and placed in either DMSO or the appropriate DMSO solution of cross-linker. The viscoelastic behaviour of the gels was measured with an ARES rheometer. The gel was placed between parallel plates and compressed with 15 g cm^2 of normal force. Oscillatory rheology data were collected at a strain of 5%.

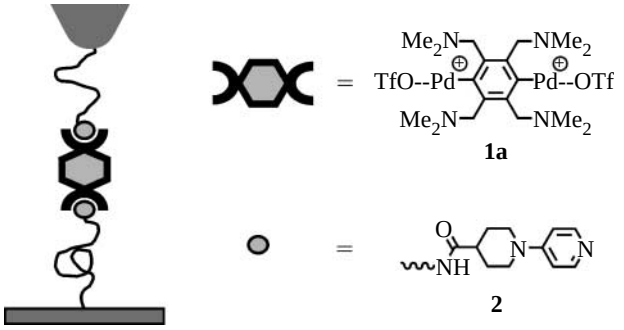

Figure 1. Pictorial representation of a single-molecule force spectroscopy experiment. PEG linkers were attached to an AFM tip and SiO_2 substrate and subsequently functionalized with **2**. A DMSO solution of **1a** was present between the tip and the surface while performing experiments.

3. RESULTS AND DISCUSSION

The response of the pincer–ligand complex **1a**·**(2)$_2$** to mechanical force was investigated with SMFS. SMFS has previously been used as a mechanical probe of a wide range of structural changes and protein folding pathways (Rief *et al.* 1997*a*,*b*; Oberhauser *et al.* 1998; Fisher *et al.* 1999; Best & Clarke 2002; Marszalek *et al.* 2002), molecular recognition events (Moy *et al.* 1994; Strunz *et al.* 1999; Kersey *et al.* 2004) and other non-covalent and coordinative-covalent interactions (Conti *et al.* 2000; Schmitt *et al.* 2000; Schonherr *et al.* 2000; Kudera *et al.* 2003; Zou *et al.* 2005*a*,*b*), including the bond dissociation of **3**·**2** (Kersey *et al.* 2006).

The experimental design is shown schematically in figure 1. An AFM tip and SiO_2 surface are functionalized with poly(ethylene glycol) chains (molecular weight approx. 3400 Da) that are functionalized on the other end with pyridine ligand **2**. The tip and SiO_2 substrate are subsequently immersed in a 0.44 mM DMSO solution of **1a**. When the tip is brought into contact with the surface and subsequently retracted, a subset of the resulting force-versus-distance curves display the mechanical signatures of specific, metal-induced bridging of the type depicted in figure 1. These force-versus-distance retraction curves comprise a nonlinear increase in force, which arises from the compliance of the poly(ethylene glycol) tethers, followed by a rupture event at a peak force (figure 2). These rupture events are centred around a separation of 40 nm, approximately twice the contour length of the 3400 Da poly (ethylene glycol) tether. In experiments where 0.44 mM **1a** is present, approximately 16% of force–separation curves display rupture events in the range of specific adhesion (30–100 nm), whereas 'non-specific' artefacts constitute less than 1% of force–separation curves without **1a**. Further evidence for the intermediacy of the **1a**·**(2)$_2$** bonds comes from competitive inhibition studies; the occurrence of apparently 'specific' events is reduced to 4% in the presence of 100 mM of the ligand DMAP, which competes with **2** for **1a**. Notably, the average force at break did not change with the added inhibitor (48 versus 50 pN at a retract velocity of approx. 230 nm s^{-1}). The irreducibility of the measured force suggests that the measurements are truly 'single molecule' in nature, a contention that is supported by

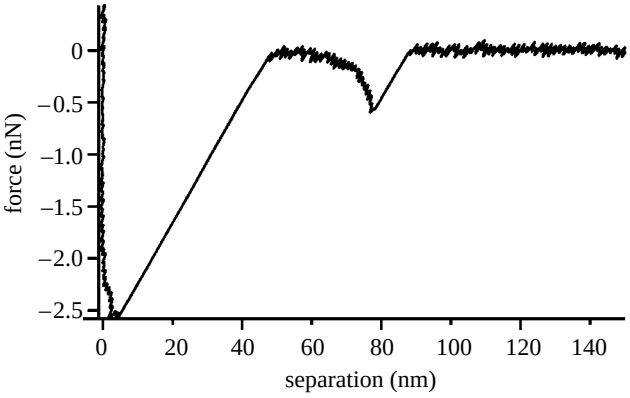

Figure 2. A representative force–separation curve showing bond rupture in **1a·2** during retraction of the AFM tip at a velocity of 2 μm s^{-1}. The stretching of the PEG chain is observed here as a nonlinear increase in force between 45 and 80 nm.

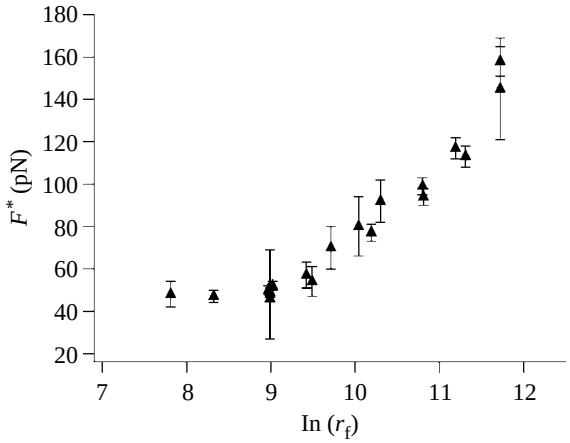

Figure 3. Dynamic force spectrum of the **1a·(2)$_2$** coordination system. Error bars reflect the standard error ($s/\sqrt{N}$) obtained from Gaussian fits to the force distributions.

the apparent elasticity of the poly(ethylene glycol) chains measured in the extension profile.

In single-molecule measurements, the force at break varies from one observation to the next. The most probable rupture force (F^*) was determined over approximately 250–600 replicate pulling experiments using the standard statistical analysis described previously. The determination of F^* was carried out for a series of tip velocities, which were converted to apparent loading rates (r_f, the rate at which the applied force increases) between 2.5 and 123 nN s^{-1} by accounting for the force constant of the AFM cantilever. For each retract velocity, the distribution of rupture forces reflects an ongoing competition in each time-interval, Δt, during which the bond can either rupture at the instantaneous force on the bond or survive until the next time increment, which leads to an increase in force that depends on the loading rate. The most probable force observed in the SMFS experiment should therefore increase with loading rate, as described in the work of Bell (1978) and Evans (1997, 2001).

The general expectation of F^* increasing monotonically with loading rate is observed (figure 3), although the dependence is not strictly logarithmic as in the case of the most commonly applied Bell–Evans formalism. In fact, for slower tip velocities, it appears that force is independent of loading rate. The deviation for the Bell–Evans equation is not surprising, and probably reflects the influence of multiple factors. First, there is a measurement bias when measuring small forces, because lower forces are more likely to be lost in background noise. Second, as noted by Evans and subsequently by others, the actual loading rate depends on the compliance not only of the AFM tip, but also of the tether linking the tip to the analyte (Evans 1997). Third, it is possible that the lower retract rates are slow relative to ligand rebinding, so that a finite force is observed (Seifert 2002; Dudko 2003; Chen 2005; Schonherr *et al.* 2005; Zou *et al.* 2005*a*,*b*).

We previously reported that the Bell–Evans treatments of SMFS data for diethylamino-functionalized pincer Pd(II) complexes are in excellent quantitative agreement with thermal, solvent-assisted dissociation rates measured on model complexes (Kersey *et al.* 2006). For comparison, we carried out the same Bell–Evans analysis on the loading rate-dependent region (high retract rates) of the SMFS data shown in figure 3. The extrapolated thermal off-rate was found to be $81 \pm 11\ s^{-1}$, and since the off-rate increases proportionally with the number of bonds in series (Evans 2001; Williams 2003; Patel *et al.* 2004), the corrected apparent thermal off-rate is $40 \pm 6\ s^{-1}$. This value is within a factor of 2 of that measured by dynamic NMR spectroscopy for a closely related model system ($85 \pm 15\ s^{-1}$; Yount 2003).

As with the previous measurements, the agreement between the extrapolated SMFS data and the dynamic NMR spectroscopy data could be fortuitous (Friedsam *et al.* 2003; Hummer & Szabo 2003). Perhaps more important than the absolute values, however, is the *relative* behaviour of the compounds. In comparing the mechanical differences of **1a·2** with those of **3·2**, we note that the stress-free, equilibrium thermodynamics of the model systems are nearly identical (1600 versus 1300 M^{-1}, respectively), but the forces required for bond rupture are lower for the faster complex **1a·(2)$_2$** than for **3·(2)$_2$** at comparable loading rates. For example, at a loading rate of approximately 30 nN s^{-1}, **3·(2)$_2$** ruptures at an average force of 164 pN, whereas **1a·(2)$_2$** ruptures at an average value of 92 pN. The bond rupture of polymer-tethered ligands under an increasing load is strongly correlated with, and it can therefore be controlled through the stress-free kinetics of the ligand dissociation. The conditions of polymer-tethered ligands in a nucleophilic solvent and a dynamic load are relevant to the behaviour of materials, such as the hybrid gels described below.

The SMFS data for **1a·(2)$_2$** complement our previous SMFS work on the related diethylamino pincer complexes **3** (Kersey *et al.* 2006), to provide a pair of compounds in which both the stress-free kinetics and the dynamic mechanical response (which is shown to be related to those kinetics) can be controlled independently of the thermodynamics of association of the metal–ligand complex. We next turned our attention to the possibility of incorporating these units

as active, stress-bearing entanglements in hybrid polymer gels. In the hybrid gels, a covalent polymer network provides a permanent structural 'memory', while an additional set of reversible cross-links would provide sacrificial cross-links that dissociate under an applied stress and then repair once the applied force is removed, to the structure defined by the covalent network.

The specific model system is a covalent gel polymerized from hydroxy-2-ethylmethacrylate (HEMA), 4-vinylpyridine (4VP) and the bis-functional cross-linker EGDMA. Discrete, transparent, elastomeric gels were prepared as described previously. To the best of our knowledge, poly-4VP-*co*-HEMA networks have not been characterized previously in water or organic solvents, although aqueous pHEMA networks, in particular, have received considerable attention. When soaked in DMSO, the cross-linked poly-4VP-*co*-HEMA network takes up roughly five times its weight in the solvent to form a stiff gel, **4**. Low-strain oscillatory rheology of discs of **4** shows a frequency-independent storage modulus G' of approximately 30 kPa.

Transient cross-links were added by placing the networks into 3 mM solutions of cross-linkers **1**. The entry of the cross-linker into the gels leads to a deepening yellow colour of the transparent disc that persists once the gels are removed from the cross-linker solution. The cross-linkers are not only chemically present, but also mechanically active in the gel. In DMSO, the hybrid gel **4**·**1b** shows frequency-dependent mechanical properties that are different from those of the parent gel **4** (figure 4). At low oscillatory frequencies, the storage modulus is that of the unmodified **4**. At oscillatory frequencies above approximately 2 rad s^{-1}, however, the storage modulus increases measurably with increasing frequency to a value of 56 kPa at 100 rad s^{-1}. The underlying relaxation is directly attributed to the dissociation and reassociation of **1b** pyridine coordination complexes by comparison with **4**·**1a**. The structural similarity of **1a** and **1b**, along with the similarities in their complexation thermodynamics to pyridine, ensures that the equilibrium structures of gels **4**·**1a** and **4**·**1b** are effectively identical. The oscillatory rheology of **4**·**1a**, however, shows a storage modulus that is nearly identical to that of **4** alone up to 100 rad s^{-1}, where a slight positive deviation occurs. The difference of a factor of approximately 50 in the observed onset is consistent with the previously reported lifetimes of the pyridine complexes of **1a** and **1b** with pyridine in DMSO.

Stronger transient cross-links can also be introduced by taking advantage of the Pt series of cross-linkers **1c** and **1d**. The cross-linker structure is again effectively identical to **1a** and **1b**, but both the previously reported thermodynamics of pyridine association (8000 and 4000 M^{-1} for **1c** and **1d**, respectively) and the lifetime of the complexes (27 and 10^3 s for **1c** and **1d**, respectively) increase relative to those of **1a** and **1b** (Yount *et al.* 2005). Each of these differences is manifested in the oscillatory rheology of the hybrid gels. The storage moduli of **4**·**1c** and **4**·**1d** (150 kPa) are higher than not only that of **4**, but also higher than the approximately 56 kPa plateau value of **4**·**1b**. The higher storage modulus is consistent with a greater number of cross-linkers in the gel due to the increased thermodynamics of pyridine coordination. The fact that the moduli of **4**·**1c** and **4**·**1d** are identical with each other is consistent with the effectively identical concentrations of **1c** and **1d**, as well as with the nearly identical thermodynamics of pyridine coordination. The lifetimes of the Pt complexes are each longer than the slowest time-scale in the oscillatory rheology (10 s), and, as expected, the moduli are frequency-independent across the range measured. The fact that the effects on mechanical properties are due to cross-linking is shown by soaking the hybrid gels in solutions containing DMAP (7 mM). Subsequent rheological measurements show that the moduli revert to those of **4**. Similarly, the rheology of the hybrid gel **4** does not change upon addition of a monometallic pincer compound; a bis-functional cross-linking, and not simple metal coordination, is required.

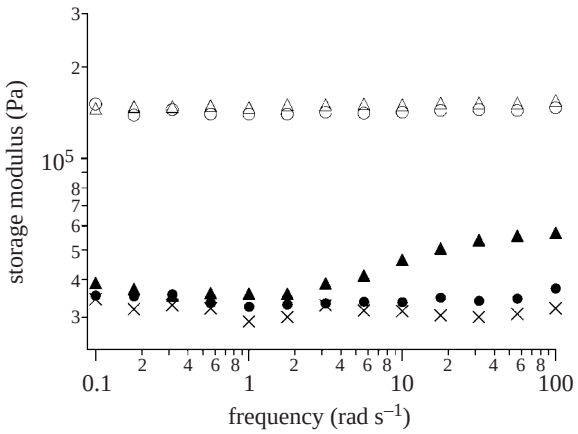

Figure 4. Storage modulus as measured by the oscillatory rheology of covalent and hybrid DMSO gels: **4**·**1d** (open circles); **4**·**1c** (open triangles); **4**·**1b** (closed triangles); **4**·**1a** (closed circles); and **4** (crosses).

The dynamic mechanical behaviour of the hybrid gels **4**·**1** shows three things. First, transient metal–pyridine coordinative bonds bear mechanical stress and contribute to the strength of the gels. Second, the transient bonds break and re-form within the hybrid gel in a manner that directly reflects the nature of the metal–ligand interaction. Third, the transient nature of the reversible interactions is present within a permanent, stiff matrix defined by the covalent EGDMA cross-links.

A combination of covalent and reversible interactions has previously been shown by Kong *et al.* (2003) to simultaneously create stiffness and toughness in gels, and it is interesting to think about the same combination in the context of self-healing materials. The SMFS data indicate that reversible cross-links ultimately might be 'programmed' to fail under stress. Material architectures in which the failure of sacrificial—but reversible—stress-bearing entanglements protects the irreversible interactions that define a macroscopic structure follow a hierarchical design found often in nature. It is also interesting to consider whether stress-induced reactions within a polymer can be used to trigger subsequent chemistry that repairs local damage.

4. CONCLUSIONS

The rational design of self-healing materials will benefit from an increased understanding of molecular, stress-induced processes within a material context. The inclusion of well-defined and specific reversible interactions in a material is an attractive strategy for engineering repair without an external stimulus, but reversibility must be combined with a permanent component that defines the desired macroscopic structure of the material. We have reported here the first members of a class of isostructural hybrid polymers possessing reversible interactions for which both the rates of stress-induced dissociation and the stress-free rates of repair can be controlled. When combined with covalent cross-links in a hybrid gel, the reversible interactions are shown to bear mechanical stress and to dissociate and re-associate in conjunction with an applied strain. The resulting material platform provides a first-generation system for evaluating structure–activity relationships in the context of self-repairing materials.

We thank S. L. Jeon for assisting with the synthesis of bismetal compounds, as well as NSF and NIH for financial support.

REFERENCES

Bell, G. I. 1978 Models for the specific adhesion of cells to cells. *Science* **200**, 618–627. (doi:10.1126/science.347575)

Best, R. B. & Clarke, J. 2002 What can atomic force microscopy tell us about protein folding? *Chem. Commun.,* 183–192. (doi:10.1039/b108159b)

Chen, H.-Y. & Chu, Y.-P. 2005 Theoretical determination of the strength of soft noncovalent molecular bonds. *Phys. Rev. E* **71**, 010901(R). (doi:10.1103/PhysRevE.71.010901)

Chen, X., Dam, M. A., Ono, K., Mal, A., Shen, H., Nutt, S. R., Sheran, K. & Wudl, F. 2002 A thermally re-mendable cross-linked polymeric material. *Science* **295**, 1698–1700. (doi:10.1126/science.1065879)

Conti, M., Falini, G. & Samori, B. 2000 How strong is the coordination bond between a histidine tag and Ni-nitrilotriacetate? An experiment of mechanochemistry on single molecules. *Angew. Chem. Int. Ed.* **39**, 215–218doi:10.1002/(SICI)1521-3773(20000103)39:1<215::AID-ANIE215>3.0.CO;2-R.

Dudko, O. K., Filippov, A. E., Klafter, J. & Urbakh, M. 2003 Beyond the conventional description of dynamic force spectroscopy of adhesion bonds. *Proc. Natl. Acad. Sci. USA* **100**, 11 378–11 381. (doi:10.1073/pnas.1534554100)

Evans, E. 2001 Probing the relation between force—lifetime— and chemistry in single molecular bonds. *Annu. Rev. Biophys. Biomol. Struct.* **30**, 105–128. (doi:10.1146/annurev.biophys.30.1.105)

Evans, E. & Ritchie, K. 1997 Dynamic strength of molecular adhesion bonds. *Biophys. J.* **72**, 1541–1555.

Fisher, T. E., Oberhauser, A. F., Carrion-Vazquez, M., Marszalek, P. E. & Fernandez, J. M. 1999 The study of protein mechanics with the atomic force microscope. *Trends Biochem. Sci.* **24**, 379–384. (doi:10.1016/S0968-0004(99)01453-X)

Friedsam, C., Wehle, A. K., Kuhner, F. & Gaub, H. E. 2003 Dynamic single-molecule force spectroscopy: bond rupture analysis with variable spacer length. *J. Phys. Condens. Matter* **15**, S1709–S1723. (doi:10.1088/0953-8984/15/18/305)

Hummer, G. & Szabo, A. 2003 Kinetics from nonequilibrium single-molecule pulling experiments. *Biophys. J.* **85**, 5–15.

Hutter, J. L. & Bechhoefer, J. 1993 Calibration of atomic-force microscope tips. *Rev. Sci. Instrum.* **64**, 1868. (doi:10.1063/1.1143970)

Janovjak, H., Struckmeier, J. & Muller, D. J. 2005 Hydrodynamic effects in fast AFM single-molecule force measurements. *Eur. Biophys. J.* **34**, 91–96. (doi:s00249-004-0430-3)

Jeon, S. L., Loveless, D. M., Yount, W. C. & Craig, S. L. In press. Thermodynamics of pyridine coordination in 1,4-phenylene bridged bimetallic (Pd, Pt) complexes containing two *N,C,N′* motifs, 1,4-M_2-[$C_6(CH_2NR_2)_4$−2,3,5,6]. *Inorg. Chem.*

Kersey, F. R., Lee, G., Marszalek, P. & Craig, S. L. 2004 Surface-to-surface bridges formed by reversibly assembled polymers. *J. Am. Chem. Soc.* **126**, 3038–3039. (doi:10.1021/ja0499501)

Kersey, F. R., Yount, W. C. & Craig, S. L. 2006 Single-molecule force spectroscopy of bimolecular reactions: system homology in the mechanical activation of ligand substitution reactions. *J. Am. Chem. Soc.* **128**, 3886–3887. (doi:10.1021/ja058516b)

Kong, H. J., Wong, E. & Mooney, D. J. 2003 Independent control of rigidity and toughness of polymeric hydrogels. *Macromolecules* **36**, 4582–4588. (doi:10.1021/ma034137w)

Kudera, M., Eschbaumer, C., Gaub, H. E. & Schubert, U. S. 2003 Analysis of metallo-supramolecular systems using single-molecule force spectroscopy. *Adv. Funct. Mater.* **13**, 615–620. (doi:10.0012/adfm.200304359)

Marszalek, P. E., Li, H., Oberhauser, A. F. & Fernandez, J. M. 2002 Chair-boat transitions in single polysaccharide molecules observed with force-ramp AFM. *Proc. Natl Acad. Sci. USA* **99**, 4278–4283. (doi:10.1073/pnas.072435699)

Moore, J. S. 1999 Supramolecular polymers. *Curr. Opin. Colloid Interface Sci.* **4**, 108–116. (doi:10.1016/S1359-0294(99)00018-7)

Moy, V. T., Florin, E. L. & Gaub, H. E. 1994 Intermolecular forces and energies between ligands and receptors. *Science* **266**, 257–259. (doi:10.1126/science.7939660)

Oberhauser, A. F., Marszalek, P. E., Erickson, H. P. & Fernandez, J. M. 1998 The molecular elasticity of the extracellular matrix protein tenascin. *Nature* **393**, 181–185. (doi:10.1038/30270)

Patel, A. B., Allen, S., Davies, M. C., Roberts, C. J., Tendler, S. J. B. & Williams, P. 2004 Influence of architecture on the kinetic stability of molecular assemblies. *J. Am. Chem. Soc.* **126**, 1318–1319. (doi:10.1021/ja0366991)

Pollino, J. M. & Weck, M. 2005 Non-covalent side-chain polymers: design principles, functionalization strategies, and perspectives. *Chem. Soc. Rev.* **34**, 193–207. (doi:10.1039/b311285n)

Pollino, J. M., Nair, K. P., Stubbs, L. P., Adams, J. & Weck, M. 2004 Cross-linked and functionalized "universal polymer backbones" via simple, rapid, and orthogonal multisite self-assembly. *Tetrahedron* **60**, 7205–7215. (doi:10.1016/j.tet.2004.05.055)

Rief, M., Gautel, M., Oesterhelt, F., Fernandez, J. M. & Gaub, H. E. 1997*a* Reversible unfolding of individual titin immunoglobulin domains by AFM. *Science* **276**, 1109–1112. (doi:10.1126/science.276.5315.1109)

Rief, M., Oesterhelt, F., Heymann, B. & Gaub, H. E. 1997*b* Single molecule force spectroscopy on polysaccharides by atomic force microscopy. *Science* **275**, 1295–1297. (doi:10.1126/science.275.5304.1295)

Schmitt, L., Ludwig, M., Gaub, H. E. & Tampé, R. 2000 A metal-chelating microscopy tip as a new toolbox for single-molecule experiments by atomic force microscopy. *Biophys. J.* **78**, 3275–3285.

Schonherr, H., Beulen, M. W. J., Bugler, J., Huskens, J., van Veggel, F. C. J. M., Reinhoudt, D. N. & Vancso, G. J. 2000 Individual supramolecular host-guest interactions studied by dynamic single molecule force spectroscopy. *J. Am. Chem. Soc.* **122**, 4963–4967. (doi:10.1021/ja994040i)

Seifert, U. 2002 Dynamic strength of adhesion molecules: role of rebinding and self-consistent rates. *Europhys. Lett.* **58**, 792–798. (doi:10.1209/epl/i2002-00101-8)

Strunz, T., Oroszlan, K., Schäfer, R. & Güntherodt, H.-J. 1999 Dynamic force spectroscopy of single DNA molecules. *Proc. Natl Acad. Sci. USA* **96**, 11 277–11 282. (doi:10.1073/pnas.96.20.11277)

Thompson, J. B., Kindt, J. H., Drake, B., Hansma, H. G., Morse, D. E. & Hansma, P. K. 2001 Bone indentation recovery time correlates with bond reforming time. *Nature* **414**, 773–776. (doi:10.1038/414773a)

Vander Wal, M., Kamper, S., Headley, J. & Sinniah, K. 2006 Effects of contact force and salt concentration on the unbinding of a DNA duplex by force spectroscopy. *Langmuir* **22**, 882–886. (doi:10.1021/la0523560)

White, S. R., Sottos, N. R., Geubelle, P. H., Moore, J. S., Kessler, M. R., Sriram, S. R., Brown, E. N. & Viswanathan, S. 2001 Autonomic healing of polymer composites. *Nature* **409**, 794–797. (doi:10.1038/35057232)

Williams, P. M. 2003 Analytical descriptions of dynamic force spectroscopy: behaviour of multiple connections. *Anal. Chim. Acta* **479**, 107–115. (doi:10.1016/S0003-2670(02)01569-6)

Yount, W. C., Juwarker, H. & Craig, S. L. 2003 Orthogonal control of dissociation dynamics relative to thermodynamics in a main-chain reversible Polymer. *J. Am. Chem. Soc.* **125**, 15 302–15 303. (doi:10.1021/ja036709y)

Yount, W. C., Loveless, D. M. & Craig, S. L. 2005 Small molecule dynamics and mechanisms underlying the macroscopic mechanical properties of coordinatively crosslinked polymer networks. *J. Am. Chem. Soc.* **127**, 14 488–14 496. (doi:10.1021/ja054298a)

Zimmerman, N., Moore, J. S. & Zimmerman, S. C. 1998 Polymer chemistry comes full circle. *Chem. Ind.*, 604–610.

Zou, S., Schonherr, H. & Vancso, G. J. 2005*a* Stretching and rupturing individual supramolecular polymer chains by AFM. *Angew. Chem. Int. Ed.* **44**, 956–959. (doi:10.1002/anie.200460963)

Zou, S., Schonherr, H. & Vancso, G. J. 2005*b* Force spectroscopy of quadruple H-bonded dimers by AFM: dynamic bond rupture and molecular time-temperature superposition. *J. Am. Chem. Soc.* **127**, 11 230–11 231. (doi:10.1021/ja0531475)